Max-Planck-Institut für Meteorologie

REPORT No. 16

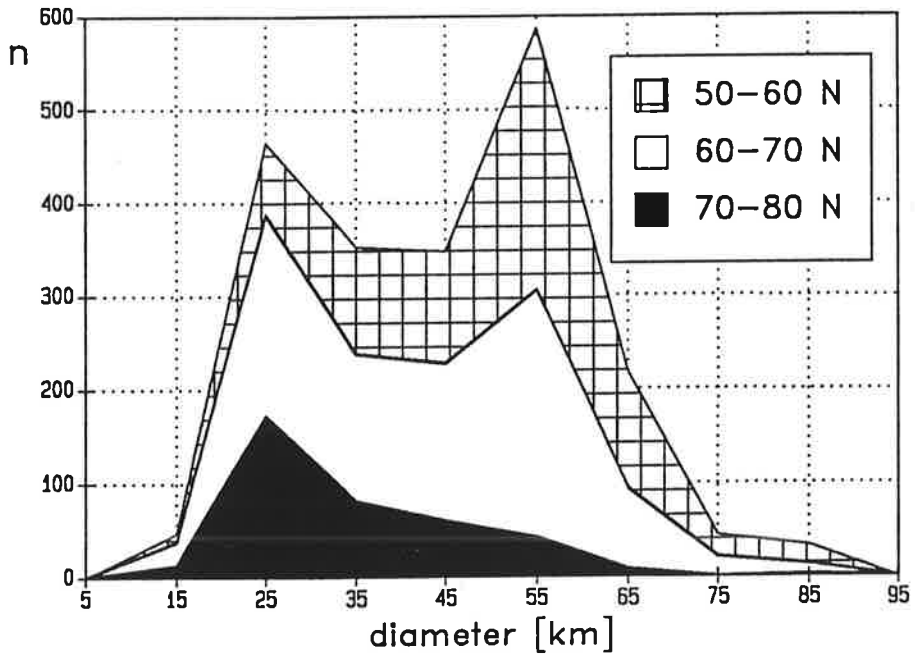

OBSERVATIONS OF CELLULAR CONVECTION OVER THE EASTERN ATLANTIC

by

STEPHAN BAKAN • ELKE SCHWARZ

HAMBURG, MARCH 1988

AUTHORS:

STEPHAN BAKAN — MAX-PLANCK-INSTITUT FÜR METEOROLOGIE

ELKE SCHWARZ — METEOROLOGISCHES INSTITUT DER UNIVERSITÄT HAMBURG
BUNDESSTRASSE 55
D - 2000 HAMBURG 13
F.R. GERMANY

MAX-PLANCK-INSTITUT
FÜR METEOROLOGIE
BUNDESSTRASSE 55
D-2000 HAMBURG 13
F.R. GERMANY

Telefon nat.: (040) 41 14 - 1
Telefon int.: + 49 40 41 14 - 1
Telex-Nr.: 211092
Telemail: MPI.METEOROLOGY
Telefax nat.: (040) 41 14 - 298
Telefax int.: + 49 40 41 14 - 298

Observations of Cellular Convection over the Eastern Atlantic

S. Bakan
Max-Planck-Institut für Meteorologie
Hamburg

E. Schwarz
Meteorologisches Institut
Universität Hamburg

Abstract

For the period 1980 to 1983 daily noon NOAA satellite images of the North-Eastern Atlantic have been examined for the appearance of organized convective cloud structures. Open cellular convection as the most abundant and best recognizable feature has been studied in more detail. This phenomenon appears in 25% of all days near Weathership M, covering on the yearly average 9%, during wintertime 13% of the North-Eastern Atlantic. Due to average air-sea temperature differences of almost -5K on the yearly average around 20% of the total heat input from sea to air in the North-East Atlantic takes place in areas of open cellular convection. An average cell diameter of 41 km is found with smaller values in the north and larger values in the south of the observation area.

The derivation of a meaningful convection height from radiosoundings turns out to be difficult, as the vertical profiles often do not exhibit well defined inversions or dry layers topping the boundary layer. Therefore, the cloud top (and, thus, convection) height was crudely estimated to be that height where the potential temperature equals the 850 hPa equivalent potential temperature.

Larger aspect ratios ($>$ 20) tend to appear with smaller convection height. Aspect ratio and convection height are almost independent of air-sea temperature difference. A stability parameter (as used in theoretical studies) shows weak dependence on air-sea temperature difference and aspect ratio and no dependence on convection height. In general, the definition of a convection height as well as related quantities as e.g. the usually applied stability ratio have to be questionned as a result of this data analysis.

1. *Introduction*

The inspection of satellite images frequently reveals organized mesoscale patterns of cumulus convection over the oceans. Most prominent are open convection cells in which a ringlike cloudy wall of 30-50 km diameter surrounds the cloud free cell center (Krueger and Fritz, 1961). While open cells mostly occur in cold air outbreaks of the midlatitude, closed convection cells prevail in subtropical subsidence areas (Agee et al., 1973; Agee, 1984). The latter consist of a shield of stratiform clouds in the center which is surrounded by a cloud free ring of several tens of kilometer diameter. Banded structures are mainly observed in winter time during cold air outflow from continents growing in horizontal spacing from a few kilometers to a few tens of kilometers several hundred kilometers downstream (Miura, 1986).

Although these phenomena have been often observed and described, a rigid assessment of their climatological importance has not yet been made. That there should be a major importance is obvious as Busack et al. (1985) find the North-Eastern Atlantic near Weathership M in roughly 20% of the time covered with open cells and as the coverage of wide areas of the subtropics with closed cells is well known (e.g. Coulmann et al., 1986). The following questions arise in this context:

1. How large are the vertical fluxes in the boundary layer in these areas of organized cellular convection and to which extent does the vertical momentum and heat transport alter the large scale structure of the lower troposphere?
2. To which extent does the related cloudiness influence the radiation balance of the boundary layer?
3. Are these influences specific to the (degree of) organization or is the obvious organization only a secondary fact in such a flow type?

An answer to these questions from the theoretical side will only be possible after a successful modelling of cellular convection which has not yet been accomplished. In the meanwhile observational data may be gathered. While the KonTur 1981 experiment yielded an intensive case study of open cellular convection (Hinzpeter, 1985; Bakan, 1985; Brümmer et al., 1985; Kruspe, Bakan, 1988) also statistical evaluation of a large number of satellite images and related synoptic data has been commenced. First results with a more limited data set showed the unexpected abundance of open cellular convection in the Eastern Atlantic and

no significant correlation of the phenomenon with large scale surface divergence (Busack et al., 1985). The essential parameter seems to be the sea-air temperature difference, which is on the average of all cellular cases around 5 K, resulting in remarkably high surface heat fluxes.

The objective of the present study was to establish a climatology of frequency and appearence of mesoscale cellular convection over the North-Eastern Atlantic from NOAA satellite images and to study the correlation with synoptic data gathered at Weathership M in the Norwegian Sea. From there surface and rawinsonde data at almost the same time as the satellite photographs are available.

The second chapter presents the data sources and the choice of derived parameters. The subsequent chapter contains the climatology of different forms of cellular convection. Chapter four deals with cell area size and cell diameter. It is followed by a chapter describing correlations with the surface data from Weathership M. Chapter six examines the rawinsonde data of the ship station and in the last chapter, finally, some conclusions are drawn.

2. Data

2.1. Data sources

The satellites of the TIROS N / NOAA series have been in orbit since 1978 (TIROS = Televison Infrared Observational Satellite, NOAA = National Oceanic and Atmospheric Administration). They fly on a sunsynchronous orbit at a height of approximately 840 km. The time for one orbital period is about 102 minutes. One of the instruments on NOAA satellites is the Advanced Very High Resolution Radiometer (AVHRR). It has five different spectral channels and the instantaneous field of view is 1.3 milliradian for all channels, which results in a resolution in the nadir of 1.1 km in each direction. Channel 1 measures in the visible range (0.55 µm - 0.68 µm), channel 2 in the near infrared (0.725 µm - 1.10 µm). The information of these two channels is used for cloud detection during day time. Channel 3 in the infrared (3.55 µm - 3.93 µm) takes over this task at night. Channel 4 (10.5 µm - 11.5 µm) and channel 5 in the thermal infrared range are used for the determination of surface temperature and water vapor in the atmosphere. For satellites with an odd number (as e.g. NOAA 7) channel 5 measures in 11.5 µm - 12.5 µm while for satellites with an even number channel

5 just repeats the data of channel 4. More detailed information about the AVHRR is given in Schwalb (1978). The data are sent in a High Resolution Picture Transmission flux and can be received when the satellite is above the horizon of a receiving station.

At the Department of Electrical Engineering and Electronics of the University of Dundee (Scotland) the original digital data of all channels of the AVHRR have been received and archived since October 1978. Photographic reproductions of the digital AVHRR data of the nearest satellite pass to Dundee are available for inspection. The resolution of the original data is degraded for those images to 4 km x 4 km at the subsatellite point. At successive days the subsatellite track varies and the satellite looks at slightly different areas, the overlapping part of which will be called central area in the following. Fig. 2.1 displays a typical NOAA AVHRR channel 4 scene as received by the University of Dundee. The area enclosed by the thick black border represents the mentioned overlap area that is contained in any of the analyzed nearest-to-Dundee passes.

The present study of cellular convection is based on the daily early afternoon AVHRR infrared and, for comparison, visible satellite image of the nearest pass to Great Britain. One image covers an area of approximately 15 million km^2. The images of 1461 days of the period 1 January 1980 through 31 December 1983 have been inspected and analyzed with the help of an interactive program on a personal computer. Only in 0.6% of all days no satellite image is available. The parameters of interest are described in the next paragraph.

2.2. Parameters

The phenomenon of interest was the convective cellular cloudiness, especially the open cells over the ocean nearby Weathership M (position: 66°N, 2°E). During the data collection the following categories were differentiated: open cells, closed cells, clouds arranged in bands. In addition to this, the cases of bandstructures ending in an area of open cells as well as open cells near Weathership M were flagged. For statistical purposes it was noted when cellular convection was detected over land in the western part of Europe. It was also noted when no satellite data were received and when absolutely no cellular convection could be detected on the whole infrared AVHRR image. Each of these cases was saved as a separate data set together with additional information on

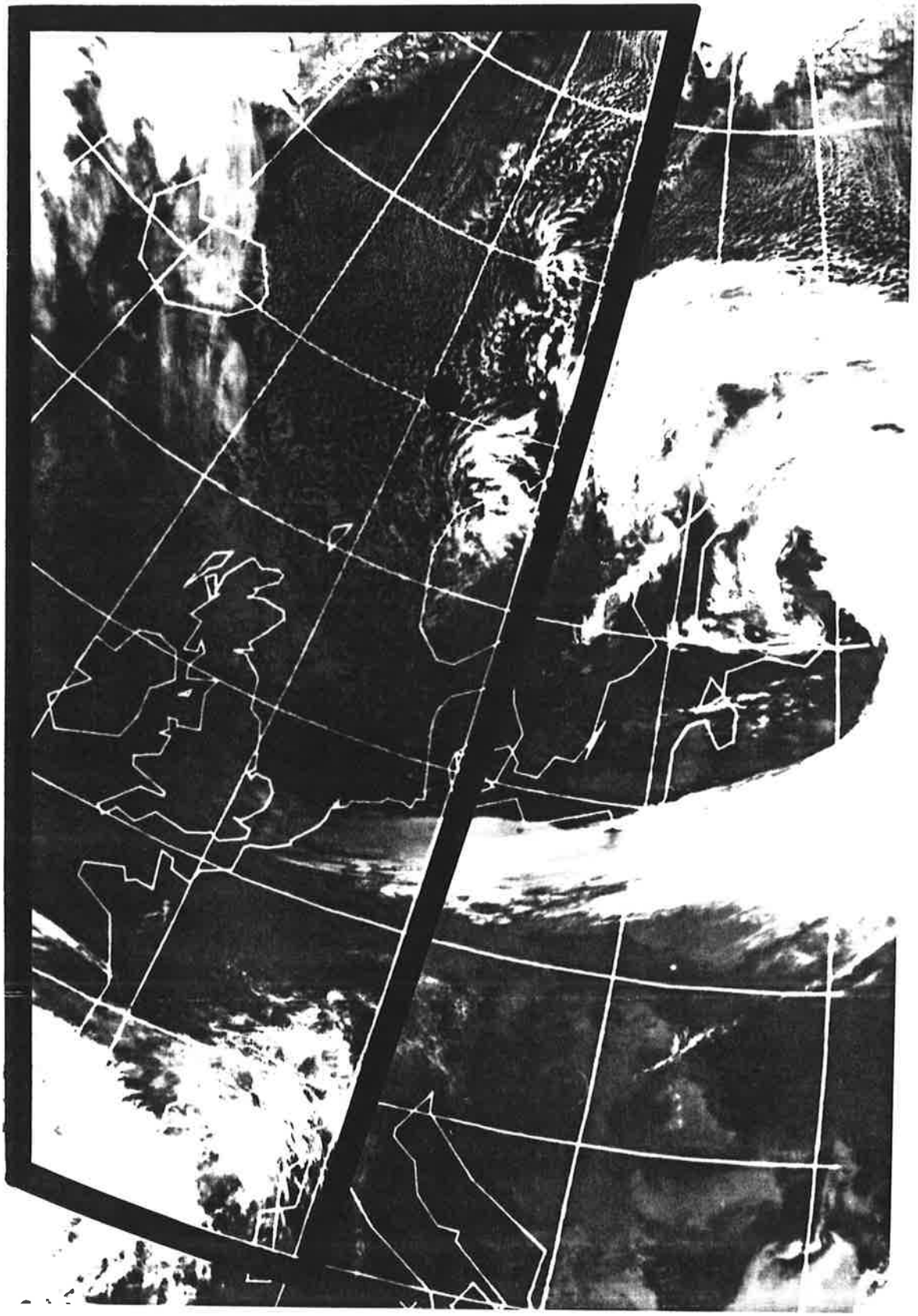

Fig. 2.1: AVHRR infrared image, channel 4, taken from NOAA-7, 23 Nov. 1983, overhead time Dundee: 13.47 UTC, the area within the black boundaries indicates the central area observable on any nearest-to-Dundee satellite pass. Additionally, the position of Weathership M (66°N, 2°E) is indicated.

derived properties of the convection as described below. Thus, from the AVHRR infrared images of 1461 days nearly 4000 data sets were determined.

If the cellular convection appeared in form of open or closed cells or bands the number of separate areas of cellular structure detectable on the satellite image was determined. For each of these areas the following information was derived with the help of a prefabricated distance grid overlay: the size, latitude and longitude of their center, and the diameter of the cells or the distance between the cloud bands. The minimum distance which can be determined is approximately 10 km. Also a crude and necessarily subjective measure of the degree of organization of the cellular convection (well, less well organized) and the height of the clouds (low, middle, high) was estimated from the images.

From Weathership M the measured surface data of wind, air and sea temperature are correlated with the data obtained during the satellite image inspection. The rawinsonde data show the vertical profiles of temperature, dewpoint and relative humidity as well as direction and speed of wind in the atmosphere in the region of Weathership M. They will also be correlated with the information of the AVHRR infrared images.

3. Climatology of mesoscale cellular convection

3.1. General findings

Surprisingly, in 92% of all days of the investigated period cellular convection could be detected in the area observed by the NOAA satellite. Only on 111 days, i.e. 8%, non of the above mentioned organized convective structures could be observed in any part of the image. Cellular convection over land in western Europe has been found on 30% of all days. This convection is not as strong and in most cases not as regular and of smaller horizontal extent as that over the ocean. The following three paragraphs will illustrate the results of the frequency of occurrences of open and closed cells, as well as those of cloud bands over sea. As an example, Fig. 2.1 shows the NOAA-7 AVHRR infrared image of the atmospheric situation on 23rd November 1983, 13.47 UTC, where many forms of convective cloudiness appear.

South of Svalbard and southeast of Greenland the cloud bands appear, which change into open cells further south. Large open cells may be seen, some of which seem to be developed into closed cells.

a. Open cells

In the daily analysis of the AVHRR infrared image one can very often detect areas of open cells. Thus most of the data sets (about 60%) describe open cellular cloudiness. The average number of registered areas of open cells per year is 583. Fig. 3.1a shows the monthly frequency of open cells from 1980 to 1983 and the corresponding average values over the investigated period. The open cellular convection has a clear annual course. July contains the minimum of convection areas with an average of 20 cases while in December the average is 80 cases.

Fig. 3.1b illustrates the latitudinal distribution of all the observed open cell areas (longitude between 30°W and 10°E). The occurrence is maximum in the northern midlatitudes and vanishes rapidly north of 70°N and south of 50°N.

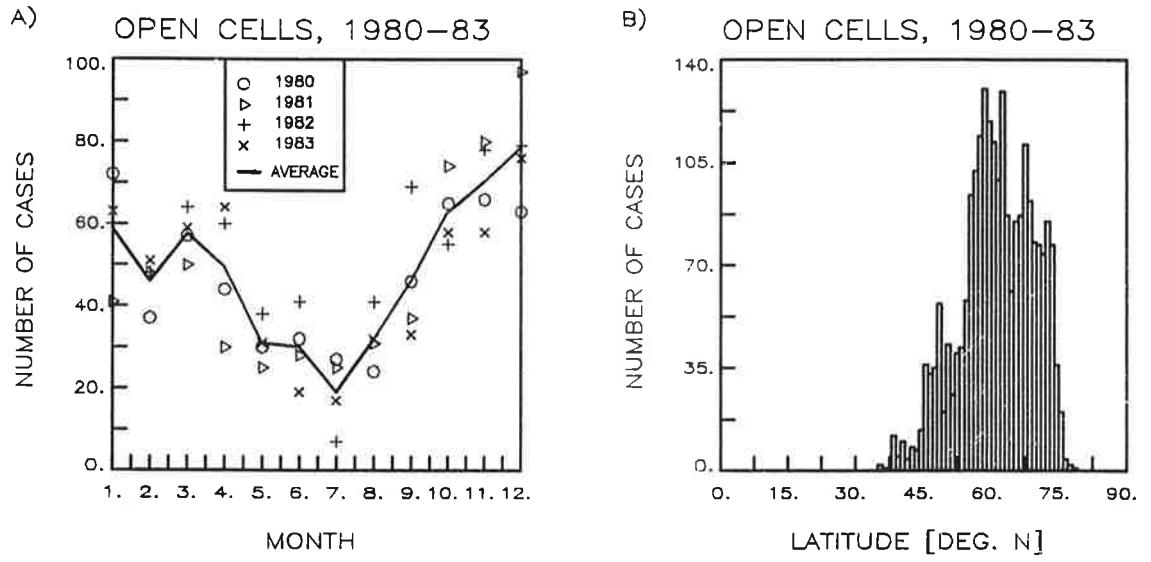

Fig. 3.1: a. Monthly frequency of occurrence of open cells for the period 1980-1983.
b. Frequency of occurrence of open cells in latitude intervals of one degree for the period 1980-1983.

b. Closed cells

Closed cells were observed ten times less than open cells. The monthly frequency of closed cells and their average value for each month is illustrated in Fig. 3.2a. No significant yearly cycle is observed. 40% of all observed closed cells of the investigated period appear in 1980.

A comparison between Fig. 3.1b and Fig. 3.2b shows that closed cells in general are found further south than open cells (between 30°N and 75°N).

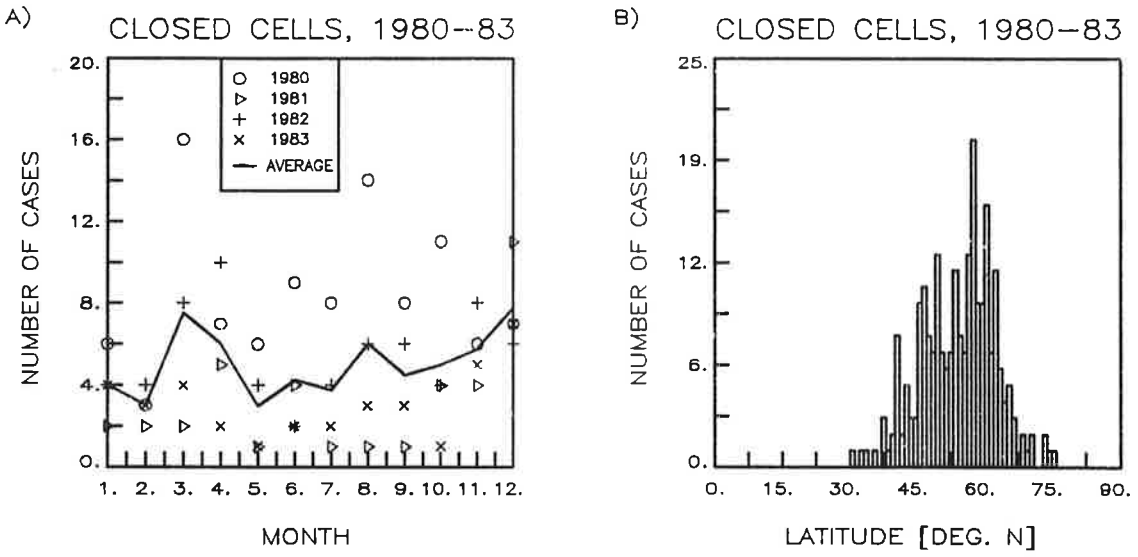

Fig. 3.2: As Fig. 3.1, however, for closed cells.

c. Banded cloud structures

10% of all cases of the whole data sets show a banded structure of cloudiness. Half of these bandstructures change over into an area of open cells downstream. The maximum of occurrences of this sort of bandstructures is found in January and December with almost 50% of all days. Fig. 3.3a shows the monthly frequency of bandstructures ending in open cells and their average values in the period 1980 to 1983. Fig. 3.3b points out that they are located further north than the open cells (between 49°N and 79°N and 30°W and 30°E). More than 80% of these bandstructures occur in latitudes north of 66°N, which is a result of their main origin in cold air flowing off ice or land.

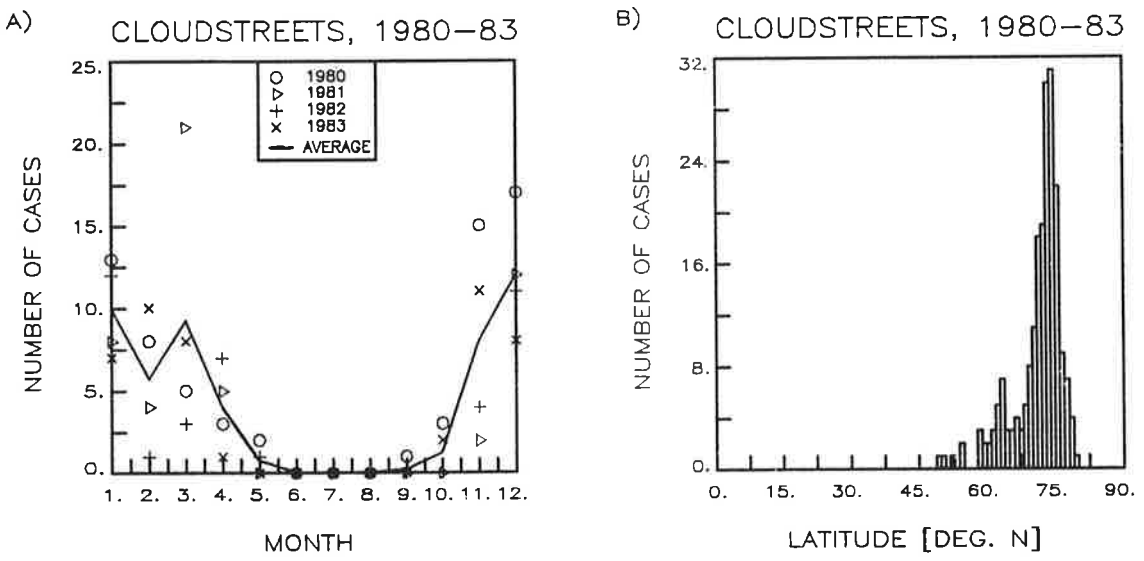

Fig. 3.3: As Fig. 3.1, however, for cloud streets.

3.2. Open cells at Weathership M

The annual course of the open cellular convection around Weathership M is similar to that of all the open cells. From 1980 to 1983 there were 354 cases of open cells detected in the region around Weathership M, i.e. at 25% of all days this kind of organization of cloudiness prevailed. About one third (101 cases) of these open cell areas reveal a strong and regular organization. Fig. 3.4 shows the monthly frequency of open cellular convection as well as the monthly average over the four years. During summer hardly any well organized cellular convection case could be detected. Except for a few cases, closed cells or banded cloud structures could not be observed during the investigated period at Weathership M.

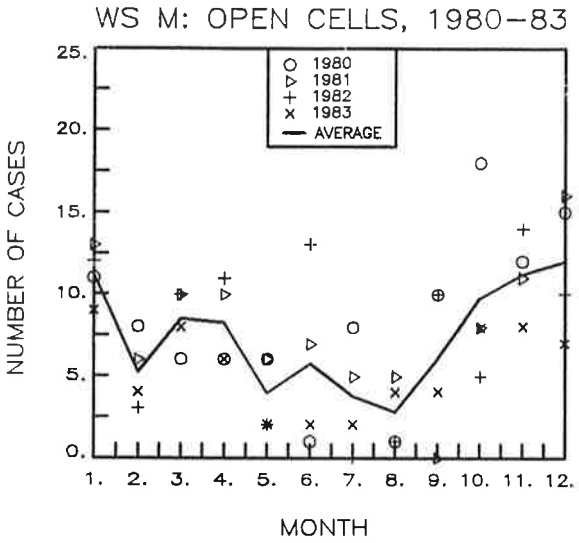

Fig. 3.4: Monthly frequency of occurrence of open cells in the region of Weathership M during the period1980 - 1983, the line indicates the average values.

4. Size characteristics of organized convection

The resolution of the available images allowed the determination of the cell diameter and the size of a continuous area of cellular convection down to a smallest dimension of about 10 km. The cell diameter is always an average value for one area. If strongly different diameters were found within one cell area it was broken down into different areas of roughly constant cell size.

4.1. Diameter of open cells

The average diameter for the open cellular convection over the investigated period 1980 to 1983 is 41 km with a standard deviation of 15 km. These results are similar to those of other authors. In the North Atlantic Krueger and Fritz (1961) found open cell diameters between 30 km and 80 km. In the Atlantic and Pacific cell diameters of 17 - 47 km were reported by Agee and Dowell (1974).

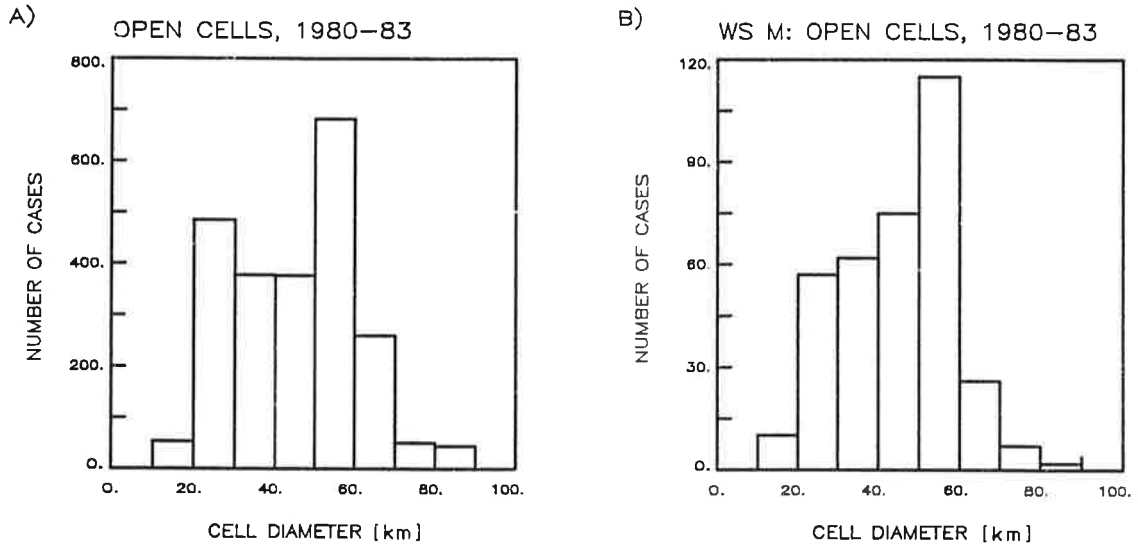

Fig. 4.1: a. Frequency of occurrence of open cells devided into several cell diameter classes of a width of 10 km for the period 1980-1983.
b. The same as a), but only for the open cells observed nearby Weathership M.

Fig. 4.1a shows the frequency distribution of all observed cell diameters which, surprisingly, exhibits two maxima. About 30% of all cases are in the 50-60 km region of cell diameter. More than 20% of the other cell diameters occur in the 20-30 km region. For comparison, the analogous diagram for the open cells near Weathership M (Fig. 4.1b) is given, which does not show such a secondary maximum at 20-30 km.

The distribution of the cell diameter depends drastically on the geographical latitude. Fig. 4.2 illustrates that in 50-60°N the 50-60 km diameters are dominant (as everywhere farther south, too) while in 70-80°N an obvious maximum diameter of 20-30 km prevails. However, no smooth transition from one of the two peak diameters to the other with increasing latitude can be observed.

This impression is emphasized in Fig. 4.3 by the latitudinal distribution of the observed centers of areas with open cells, where the ordinate represents the relative abundance of a certain diameter class in a latitude interval of 1 deg. Smaller cells (20-30 km) make up for more than 40% of all cell cases in the

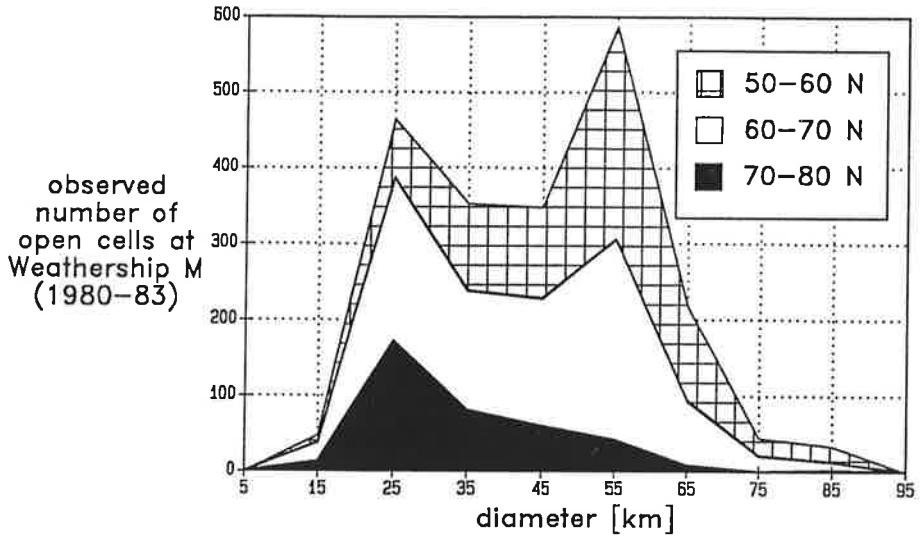

Fig. 4.2: Cumulative number distribution of open cells in the years 1980 - 1983 versus their diameter (class width ± 5 km around the indicated abszissa value) for different latitude intervals.

latitude interval north of 70°N. Areas with cell diameters of 50-60 km, on the other hand, appear mainly in lower latitudes where their share is up to 50%.

4.2. Size of open cell areas

Fig. 4.4 shows the frequency distribution of the size of whole areas with open cellular convection. While the maximum frequency of area size is between 1 and $2 \cdot 10^5$ km^2 the mean size of the open cell areas is $3.4 \cdot 10^5$ km^2 with a standard deviation of the same order. Larger areas are rare. From the average number of observed cell areas per satellite image in the overlapping central area an average coverage with cellular regions of 9%, in wintertime of 13% is found.

4.3. Closed cells and bandstructures

The diameter of closed cells has an average value of 53 km with a standard deviation of 17 km, thus closed cells are larger than open cells. On the other hand, the average size of closed cell areas is $2.6 \cdot 10^5$ km^2 and therefore smaller than that of open cells.

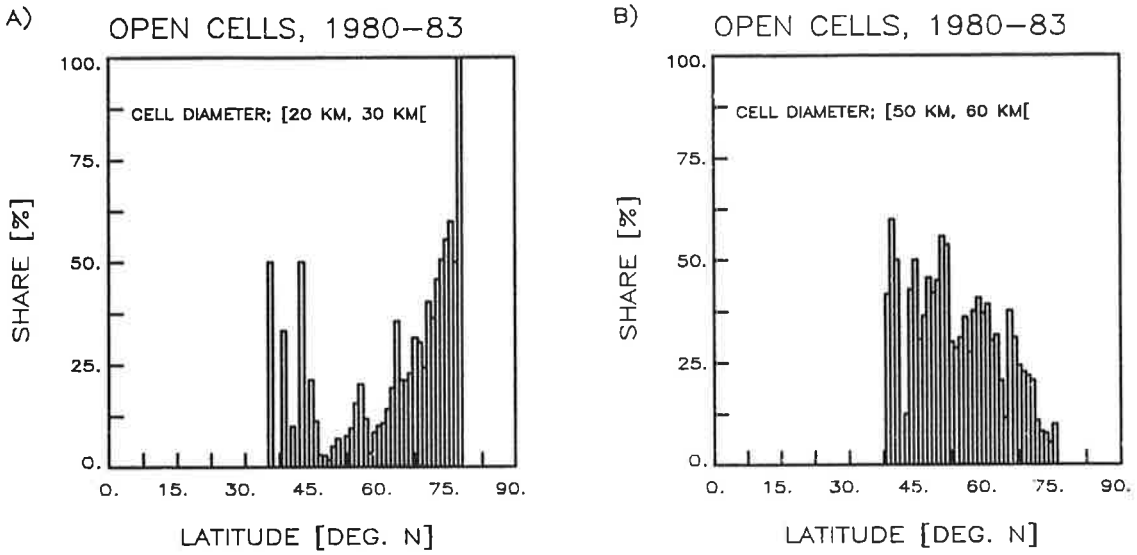

Fig. 4.3: Contribution (in %) of open cells of a given diameter class to all observed open cells in the same latitude interval of 1° width.
a. cell diameter: 20-30 km
b. cell diameter: 50-60 km.

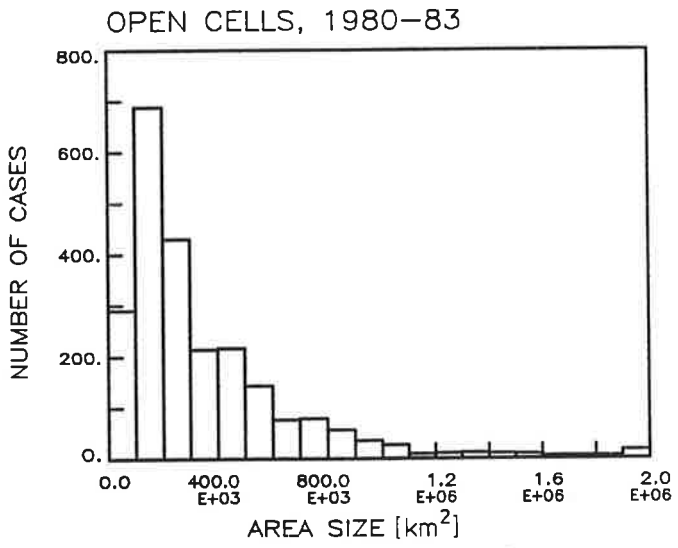

Fig. 4.4: Distribution of the open cell area size (intervall width: 10^5 km^2) during the period1980-1983. The interval 1.9 - 2.0 · 10^6 km^2 contains all larger areas, too.

For bandstructures the average distance between the clouds is calculated to be 14 km. This is a doubtful value as it is very near to the resolution limit of the satellite image and human eye. The mean area size of bandstructures is found to be also around $2 \cdot 10^5$ km^2.

5. *Surface data during cellular convection*

At Weathership M (the rawinsonde station in the Norwegian Sea) surface observations are made in at least a three-hour sequence. To correlate the data of these measurements with the satellite data, the 15.00 UTC surface data were taken which are closest to the early afternoon satellite pass. Due to the small number of other phenomena (see ch. 3.2) surface data only for open cellular convection are discussed in the following.

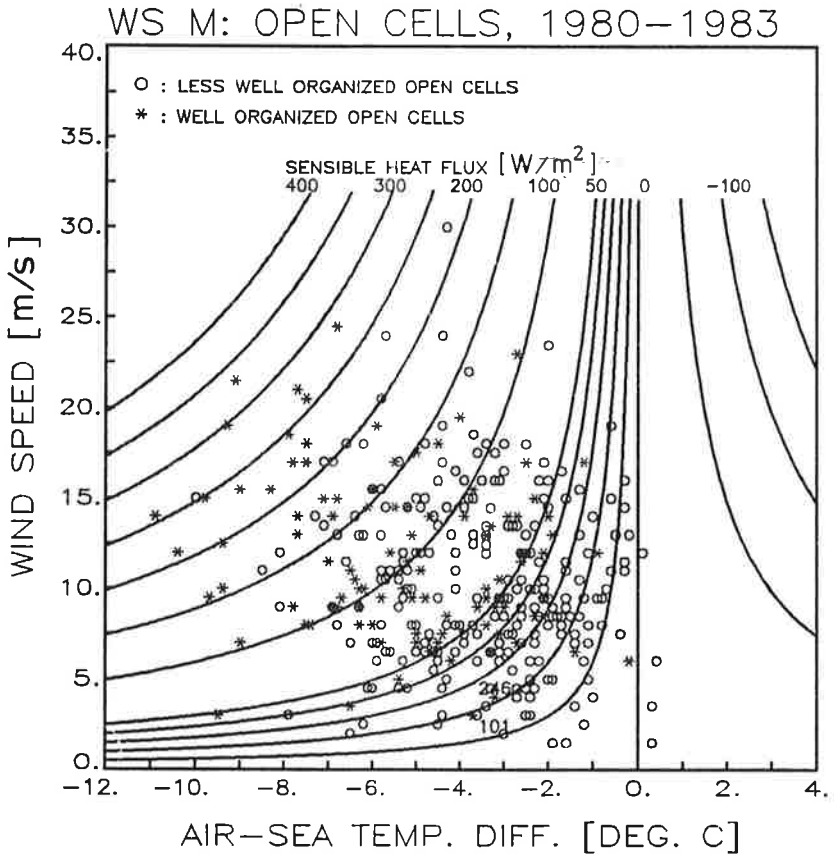

Fig. 5.1: Scatterdiagram of wind speed versus air-sea temperature difference for the well organized (*) and less well organized (o) open cell cases at Weathership M during 1980-1983. Additionally the isolines of the sensible heat flux are shown.

5.1. Air-sea temperature difference

Fig. 5.1 shows a scatter diagram of wind speed versus air-sea temperature difference in 347 cases of regular organized (101 cases) and less regular organized (246 cases) open cellular convection. For the regular organized open cells the average of wind velocity is 11.8 m/s with a standard deviation of 4.5 m/s and the average air-sea temperature difference is -5.3 ± 2.4°C corresponding to a sensible heat flux of 110 ± 73 W/m^2. For the less regular organized cell cases the average wind velocity is only slightly different (10.4 ± 4.7 m/s) while the averaged air-sea temperature difference is -3.6 ± 1.9 °C and the sensible heat flux is 65 ± 50 W/m^2. Busack et al. (1985) found for all detected convection cases an average value of -4.7 ± 2.4°C which lies well within the present range of temperature differences. On the average, the wind velocity increases with decreasing air-sea temperature difference. This may be due to the warming of slowly transported air masses by convection.

In Fig. 5.2 the appearance of cellular convection at different values of the total (bulk) surface heat flux is indicated. Average total heat fluxes of around 200 W/m^2, with occasional values larger than 500 W/m^2, hint at the importance of the phenomenon for the atmospheric heat budget.

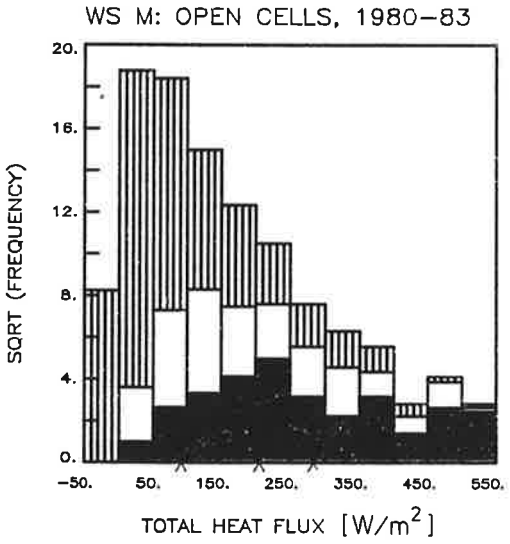

Fig. 5.2: Distribution of the total heat flux in intervals of 50 W/m^2 nearby Weathership M for the period 1980-1983
■ :well organized open cells,
□: less well organized cells,
Ⅲ: all other (nonconvective) cases.
The arrows at the abszissa axis indicate the average heat flux values from right to left in the above sequence.

For comparison also the data for non-convective cases are shown. Again a tendency may be found for the better cellular organization to occur with larger heat fluxes from sea to air.

5.2 Cell size

As shown in ch. 4.1 different cell size distributions are observed north of 70°N and south of 60°N. It could be suspected that this difference is reflected in different surface conditions. Although the smaller size peak in the distribution at Weathership M does not show up, surface data are analyzed for a few different size classes.

For the following considerations only the data of the winter months (i.e. January to April and October to December) 1980 to 1983 are used which contain most of the cell cases (83 well organized, 178 less organized).

Table 5.1 summarizes the average wind velocity and air-sea temperature difference for various size classes of open convection cells. The wind speed of 10-14 m/s does not correlate with the cell diameter. But the absolute value of air-sea temperature difference turns out to be largest for diameters around 40 km,

Diameter [km]	D < 30	30 < = D < 40	40 < = D < 50	50 < = D < 60	60 < = D	Total
Number of cases	41	39	54	98	29	261
|v| [m/s]	13.3 ± 5.1	11.8 ± 4.3	12.7 ± 4.8	10.5 ± 4.7	9.7 ± 4.2	11.5 ± 4.8
$T_A - T_W$ [°C]	- 3.9 ± 2.1	- 5.4 ± 1.8	- 5.5 ± 2.3	- 4.7 ± 2.0	- 3.1 ± 1.8	- 4.7 ± 2.2
T_A [°C]	3.3 ± 2.6	1.3 ± 2.6	1.2 ± 2.9	1.8 ± 2.2	3.6 ± 2.0	2.0 ± 2.6
T_W [°C]	7.2 ± 1.3	6.7 ± 1.1	6.8 ± 1.2	6.4 ± 0.9	6.7 ± 0.9	6.7 ± 1.1
T_D [°C]	- 0.9 ± 3.7	- 3.8 ± 3.7	- 2.9 ± 3.3	- 2.9 ± 2.5	- 1.1 ± 2.3	- 2.5 ± 3.2
$T_A - T_D$ [°C]	4.1 ± 2.1	5.1 ± 2.0	4.1 ± 1.6	4.7 ± 2.0	4.7 ± 1.3	4.5 ± 1.9
SHF [W/m²]	91.3 ± 68.3	111.7 ± 61.6	118.6 ± 72.4	82.6 ± 51.5	45.2 ± 28.9	91.6 ± 62.9
LE [W/m²]	150.8 ± 76.7	157.5 ± 70.5	157.5 ± 68.3	124.4 ± 60.1	101.8 ± 50.4	137.8 ± 68.2
SHF + LE [W/m²]	242.0 ± 138.9	269.1 ± 128.2	276.2 ± 135.1	207.0 ± 106.2	147.0 ± 73.3	229.4 ± 125.5
SHF/LE	0.6 ± 0.3	0.7 ± 0.2	0.7 ± 0.2	0.6 ± 0.2	0.5 ± 0.2	0.6 ± 0.3

Table 5.1: Average values and their standard deviation for several meteorological parameters (wind speed |v|; air, sea surface, dew point temperature T_A, T_W, T_D, respectively; sensible, latent heat flux SHF, LE, respectively) in different cell diameter classes as well as the average over all diameter classes, observed at Weathership M during wintertime 1980-1983 (i.e. January to April and October to December).

falling off considerably towards smaller and larger diameters. The sensible (SHF) and latent (LE) heat flux are calculated by the bulk aerodynamic formula with a heat and moisture transfer coefficient of 0.0013. The sensible heat flux is for large cells only about 45 W/m2. For all other cases the mean value of this parameter lies between 80 and 120 W/m2.

Fig. 5.3 shows the dependence of cell diameter on wind direction. Most of the convection cells are found with southbound winds. The average wind direction shows a tendency to increase with increasing cell size. This could be an effect of varying distance of Weathership M from the ice (and land) boundary for different directions as may be inferred from Fig. 5.3, where these distances are shown in addition.

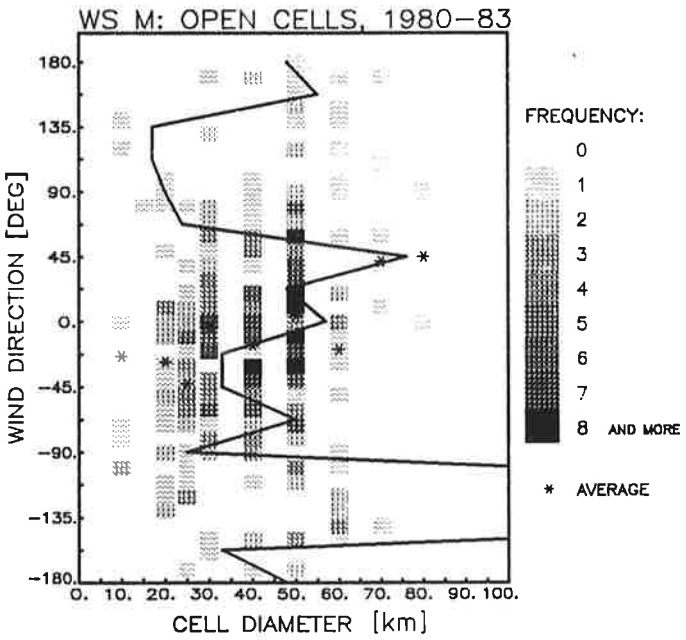

Fig. 5.3: Occurrence frequency of various combinations of cell diameter and wind direction. Stars indicate the average wind direction for each cell diameter. Additionally, the line displays the distance of Weathership M from the ice (or land) boundary in that direction from which the wind blows (to get distances in km multiply abscissa values by 25).

6. *Atmospheric structure during cellular convection*

For the present investigation the daily noon rawinsonde data from Weathership M in the Norwegian Sea between 1980 and 1981 were available, providing vertical profiles of temperature, dewpoint, relative humidity, wind direction, and wind velocity at standard levels and at levels with remarkable changes of any of these quantities.

After a check for reliability of the data only 82 of 199 days of open cells observed nearby Weathership M in 1980 and 1981 were selected for further evaluation. Fig. 6.1 shows the time series of the equivalent potential temperature at 850 hPa. The average value of 290.6 K is subtracted as well as the annual cycle, the amplitude (10.1 K) of which has been determined by a least squares fit of a cosine fixed in phase. Almost all open cellular convection cases show a negative deviation from the mean value, which reflects essentially the large air-sea temperature difference during their appearance.

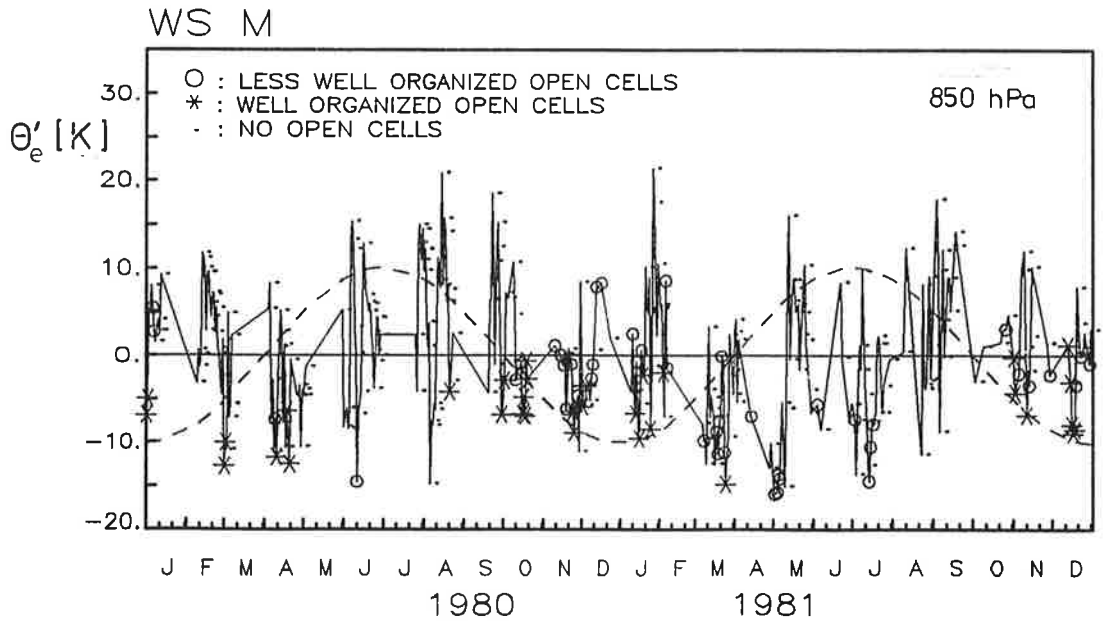

Fig. 6.1: Time series of the equivalent potential temperature minus the average value (290.6 K) and the annual cycle (calculated amplitude: 10.1 K and given cosine phase). The latter is represented by the dashed line.

Potential temperature profiles are generally found to be stably stratified throughout the troposphere. Nevertheless, the profiles show very different inversion heights and strengths (Fig. 6.2). Most remarkable seems the fact, that in many cases such an inversion is completely missing. Till now none of the observed cell characteristics could be attributed to these different inversion types.

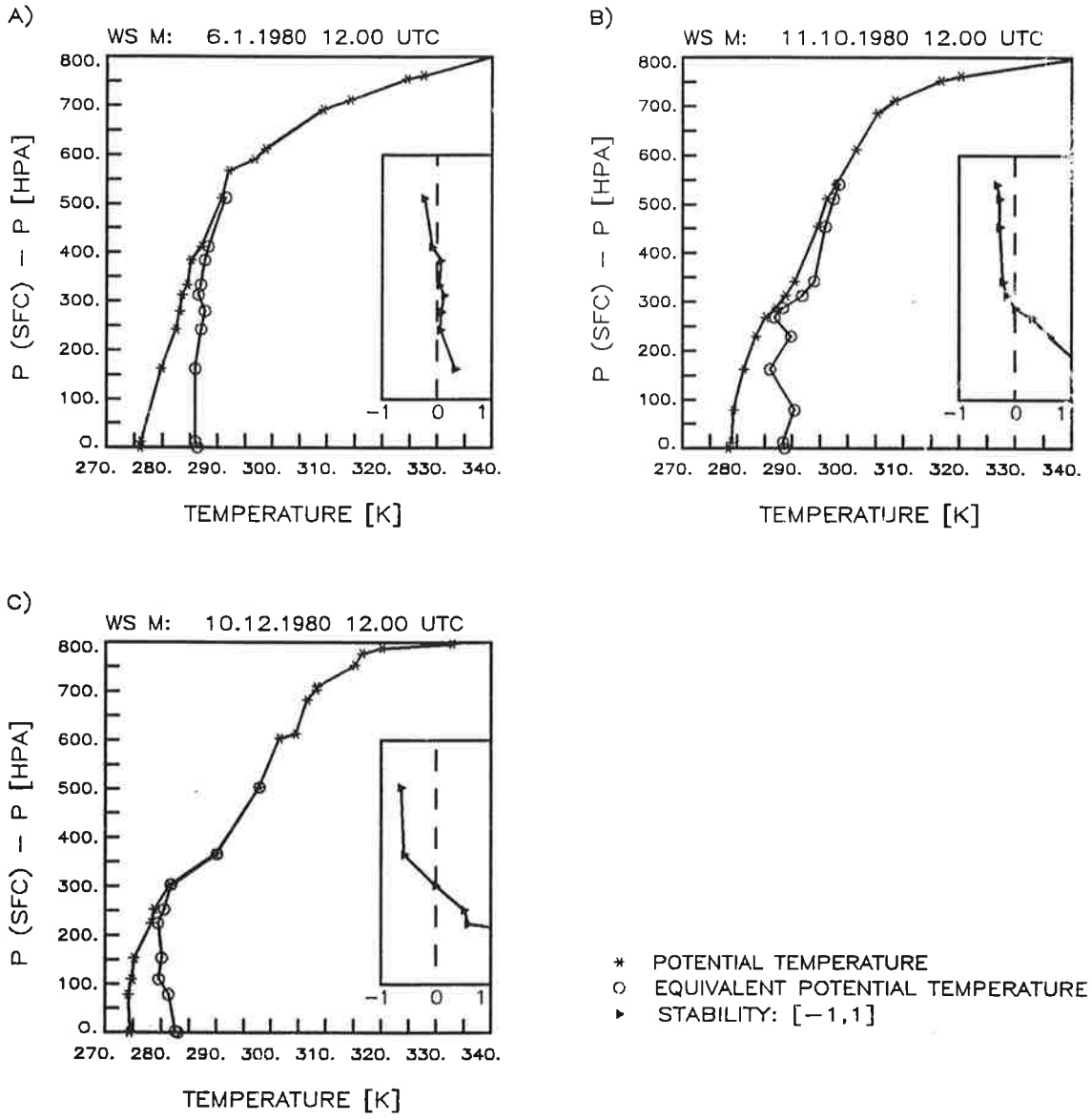

Fig. 6.2: Profiles of the potential (*) and the equivalent potential temperature (o). The height scale is given by the difference of surface and actual pressure which is almost proportional to height (with a factor of ~9) below 3000 m. At the right hand side a profile of the stability parameter (see ch. 6.2) near the inversion is added.

6.1. Convection height and aspect ratio

In theoretical studies of organized convection the layer depth either by itself or in derived quantities (e.g. aspect ratio, Rayleigh number) plays an important role. Therefore, the convection height would be a primary quantity to derive from data for intercomparison with model results. But due to the mentioned lack of a definite temperature inversion the determination of a characteristic height scale poses problems. Kruspe and Bakan (1988) encountered this problem also in the analysis of KonTur 1981 data. From their experience, the reduction of relative humidity from values >70% within the convection layer to values <50% above should yield additional valuable information to determine convection heights. But in contrast to the single radiosoundings of the present study, they have averages from 4 stations with a mutual distance of around 100 km and time periods between successive launches down to 90 minutes for additional averaging available. Single radiosoundings show a considerable scatter in the moisture record near the cloud top level indicating problems with the use of a simple relative humidity criterion in our case. Therefore, we used the following objective criterion to derive convection height without manual intervention:
As equivalent-potential temperature Θ_e contains sensible and latent heat it represents the total buoyancy of an air parcel that rises high enough in the atmosphere to release all of its latent heat. As this quantity is nearly conserved in an ascending air parcel, the level of intersection with the environmental potential temperature profile $\Theta(z)$ should characterize the convection height. Due to the fact that in reality not all the latent heat can be made available for buoyancy and due to the neglection of mixing with the environment, the resulting height should be an upper limit to the real values. The lower the resulting height the less latent heat could be released in a real ascent, but, in contrast, the less mixture had to be accounted for. On the other hand, the effect of overshooting and of accidental positive deviations of Θ_e in the starting level of the parcel could be thought of being included by just using the sketched simple procedure. Experience shows the vertical profile of Θ_e to decrease from the near surface value to a minimum that is usually found around 850 hPa in cellular convective situations. To reduce a possible overestimation not the surface but the 850 hPa value of Θ_e has been used to estimate convection height. This technique has proven quite reliable as compared to maximum cloud height esti-

mations from aircraft during KonTur 1981 as shown in Fig. 6.3. A tendency towards slight overestimation of smaller cloud top heights may be seen as well as a scatter of the estimates of less than 500 m. Nevertheless, these few data points do not allow a general justification of the mentioned procedure. Insofar the following evaluation has to be considered as preliminary.

Fig. 6.4 shows the convection height versus the air-sea temperature difference and versus the aspect ratio and the mutual dependence of the two latter quantities. Due to the considerable scatter of results in Fig. 6.4a it is not allowed to assume any correlation between convection height and air-sea temperature difference. Fig. 6.4b shows that most cases correspond to aspect ratios around 10-20. Rather few cases reveal aspect ratios >20, but in these cases a reduced scatter and a clear tendency towards smaller convection heights is obvious. This corresponds to the tendency observed by Agee (1976), although the scatter in the present study is considerably higher. Whether the apparent reduction of convection heights towards smaller aspect ratios (<10) is significant is not clear as these cases belong to diameters at the limit of detection by eye in the satellite

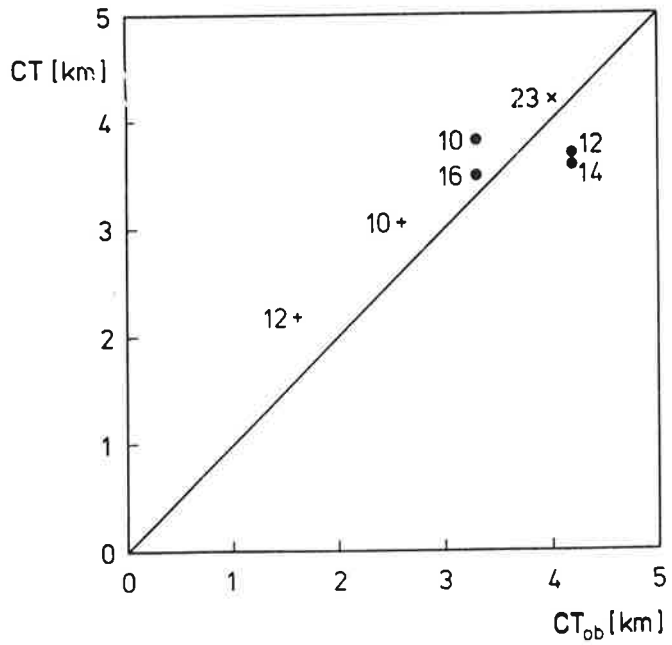

Fig. 6.3: Comparison of cloud top level CT in convective situations as determined by $\Theta(CT) = \Theta_e$ (850 hPa) with airplane observations during first (x) and second (•) phase of KonTur 1981 and during KONTROL 1985 (+).

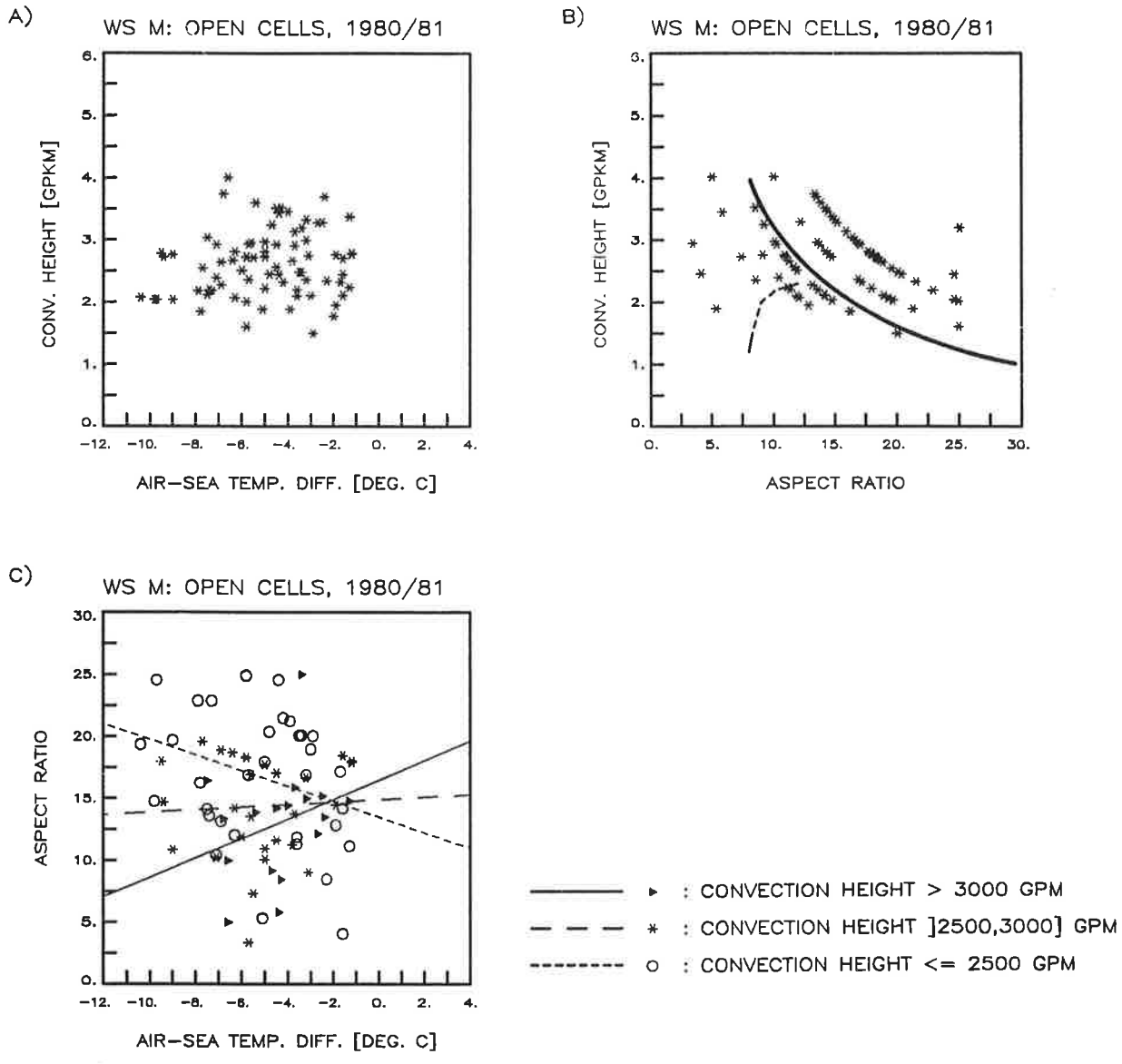

Fig. 6.4: Convection height versus air-sea temperature difference (a) and versus aspect ratio (b). The solid line in (b) represents results by Agee (1976) and the dashed line those from Miura (1986). Aspect ratio versus air-sea temperature difference is plotted in (c) together with regression lines for three convection height classes.

images. But it is interesting to note that Miura's (1986) results of open cells in cold air outbreaks over the Chinese Sea show a similar behaviour, although at smaller heights.

Fig. 6.4c, finally, shows that between aspect ratio and air-sea temperature difference a clear correlation is lacking for cases with convection heights > 2500 m. For smaller heights, however, an increase of aspect ratio with increasing water-air temperature difference is revealed.

6.2. Stratification in the convection layer

Another essential parameter of the convection problem is the layer stability. In the analysis of classical laboratory convection the Rayleigh number represents this quantity. In more recent papers, that include latent heat release, an additional stability parameter has been used to account for the moist adiabatic stratification (e.g. van Delden (1986)):

$$\left(\frac{\partial T}{\partial z} - \left. \frac{\partial T}{\partial z} \right|_m \right) / \left(\left. \frac{\partial T}{\partial z} \right|_d - \frac{\partial T}{\partial z} \right)$$

Here the indices m and d stand for moist and dry adiabatic temperature gradients, respectively. This stability parameter may also be expressed, using the equivalent potential temperature, by

$$- \frac{\partial \Theta_{es}}{\partial z} / \frac{\partial \Theta}{\partial z} \quad .$$

In analogy to Miura the discrete version $\Delta \Theta_{es}/\Delta\Theta$ of this above expression is determined by using differences between convection height and surface. Fig. 6.5 shows the stability ratio for three different height classes versus air-sea temperature difference (a), versus convection height (b), and versus aspect ratio (c). Although the scatter of these results is rather large, an increase of stability with increasing sea-air temperature and with increasing aspect ratio is revealed. It is remarkable that the results deviate considerably from those obtained by Miura, who, for example, found no negative stability values at all. Also he derived increasing stability ratio with decreasing aspect ratio.

These differences may be attributable to Miura's different method to derive cloud top heights, which he estimated from infrared satellite images. It is stated,

that the cloud top temperature estimate leads to cloud top heights marginally different from the inversion base height, but unfortunately, nothing is said about the details of the height derivation procedure.

On the other hand, the value of the stability ratio is extremely sensitive to the choice of convection height.Fig. 6.2 shows that this parameter may vary between + 1 and -1 within a few hundred meters height near the inversion. Tests with different upper or lower heights for the stability derivation show that the resulting parameter values are similarly variable and unreliable. Therefore, the choice of convection height is crucial for the stability values derived and may even have consequences for their eventual dependency on other parameters.

As a consequence, it must be assumed that either the chosen approximation to the stability parameter definition is not well justified or that the stability parameter as such turns out to be not a primary parameter to classify cellular convective situations. This question is of major importance as a similar stability parameter has been used recently to explain the observed cell broadening in cold air outbreaks (Chlond, 1988). But as these modelling approaches usually contain highly idealized approximations to the atmospheric boundary layer it may well be, that parameters governing these model calculations pertain only to special situations in the real atmosphere. It could be speculated that only situations with a very well expressed temperature inversion capping the boundary layer may be described by such a modelling approach, containing a rigid upper lid and invariable boundary temperatures. But as has been shown in ch. 6.1 (Fig. 6.2) the present data set contains only a very few cases with well expressed inversions, which may result in different governing parameters or in different dependences not yet revealed by modells.

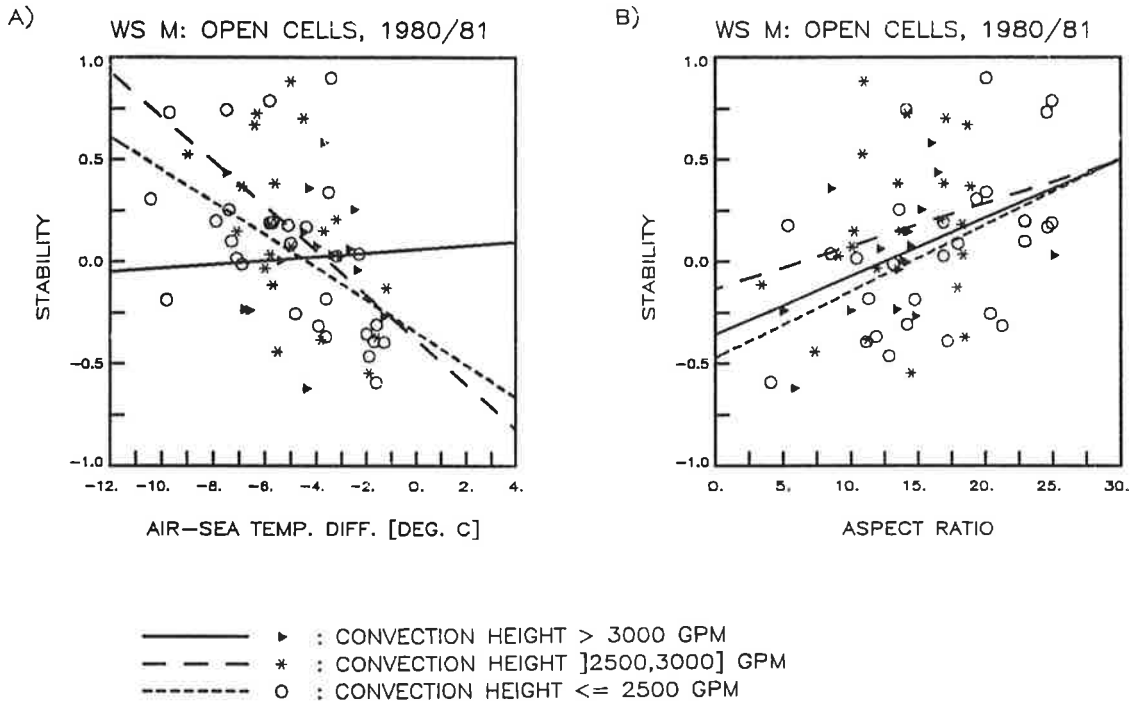

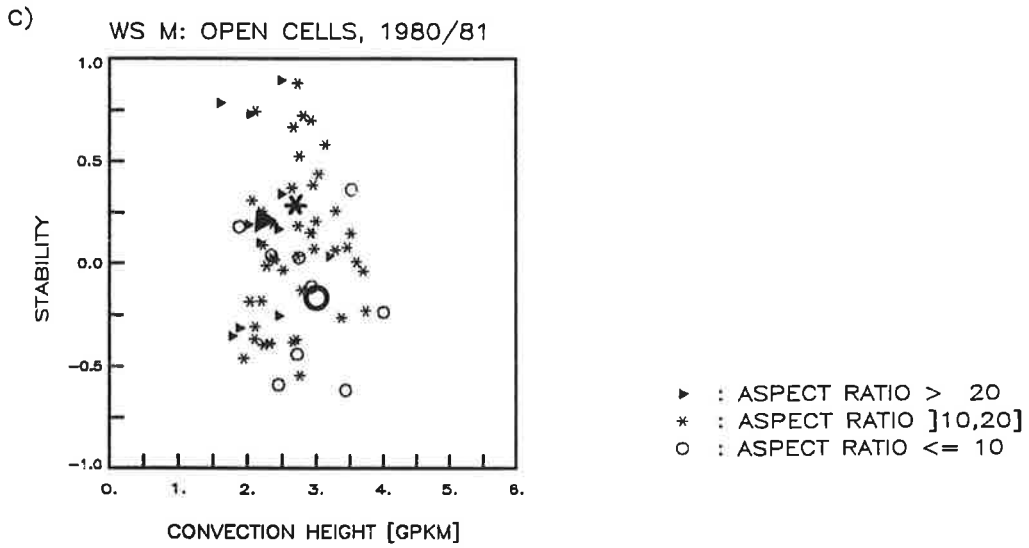

Fig. 6.5: Stability versus air-sea temperature difference (a), aspect ratio (b), and convection height (c) for open cell cases near Weathership M in 1980 and 1981. Regression lines for several convection height classes are shown in (a) and (b). Averages of aspect ratio classes are added in (c).

7. *Conclusion*

In conclusion the present study revealed a number of interesting details and, at the same time, questions on the properties of open cellular convection being based on a rather big number of observations. As could be expected from the statistical approach, a rather big scatter of data obscurs a number of possible relations among parameters of relevance. For example, it seems surprising, that there should be no correlation between convection height and sea surface temperature.

The interesting facts from these study are the following:

1. While on roughly 25% of the days open cellular convection is observed near Weathership M, on the yearly average 9% of the total area of the NE-Atlantic is covered by convection cells.
2. As the average sea-air temperature difference is around 5K on the yearly average around 20% of the total heat input from sea to air in the NE-Atlantic, occurs in areas of open cellular convection.
3. The average cell diameter is found to be 41 km with the most abundant cell diameter of 20-30 km south of 60°N and, on the other hand, of 50-60 km north of 70°N. From the results at Weathership M a dependence on the distance from the coast line as well as on air-sea temperature difference is indicated. This results in rather small cell sizes in the North-Eastern Atlantic, where distances from the ice boundary are generally small.
4. The derivation of a meaningful convection height from radiosoundings turns out to be difficult as the vertical profiles often do not exhibit well expressed inversions or dry layers topping the boundary layer. The chosen Θ_e (850 hPa) criterion to estimate cloud top height in convective situations seems to be a compromise between physical reasoning and computational efficiency. It is not obvious, however, that the cloud top height should be a good representation of the well defined convection heights in theoretical and laboratory modelling. Nevertheless, lacking a better definition, this quantity is taken to derive aspect ratio and further quantities, that describe vertical structure.
5. Convection height as well as aspect ratio are almost independent of air-sea temperature difference.
6. Comparison of a stability parameter as used in theoretical studies of organized convection with observations by Miura (1986) shows weak, but different dependency of this quantity on convection height and aspect ratio. In

studying the reasons for the differences basic difficulties with the estimation of the stability parameter for a single convective situation appear that have to be resolved in future.

Acknowledgement

The surface synoptic and rawinsonde data of Weathership M were obtained from the German weather service (Deutscher Wetterdienst, Offenbach). The authors wish to thank B. Zinecker and U. Kircher for typing and editing the manuscript.

8. Literature

Agee, E.M. (1976):

Observational evidence of cell flatness as a function of convective depth and eddy anisotropy. J. Meteorol. Soc. Japan, 54, 68-71.

Agee, E.M. (1984):

Observations from space and thermal convection: A historic perspective. Bull. Amer. Meteor. Soc., 65, 938-949.

Agee, E.M., K.E. Dowell (1974):

Observational studies of mesoscale cellular convection. J. Appl. Meteor., 13, 46-53.

Agee, E.M., T.S. Chen, K.E. Dowell (1973):

A review of mesoscale cellular convection. Bull. Amer. Meteor. Soc., 54, 1004-1012.

Bakan, S. (1985):

On the structure of open cellular convection as revealed by time series of surface observations: A case study. Beitr. Phys. Atmosph., 58, 11-16.

Brümmer, B., S. Bakan, H. Hinzpeter (1985):

KonTur: Observations of cloud streets and open cellular structures. Dyn. Atm. Oc., 9, 281-296.

Busack, B., S. Bakan, H. Luthardt (1985):

Surface conditions during mesoscale cellular convection. Beitr. Phys. Atmosph., 58, 4-10.

Chlond, A. (1988):

Numerical and analytical studies of diabatic heating effect upon flatness of boundary layer rolls. Submitted to Beitr. Phys. Atmosph.

Coulmann, S., S. Bakan, H. Hinzpeter (1986):

A cloud climatology for the South Atlantic derived from METEOSAT I images. Tellus 38A, 402-461.

Hinzpeter, H. (1985):

KonTur-Results. Beitr. Phys. Atmosph., 58, 1-3.

Krueger, A.F., S. Fritz (1961):

Cellular convection patterns revealed by Tiros 1. Tellus, 13, 1-7.

Kruspe, G., S. Bakan (1988):

The atmospheric structure in open cellular conditions during KonTur 1981. Report, Max-Planck-Institut für Meteorologie, Hamburg.

Miura, Y. (1986):

Aspect ratios of longitudinal rolls and convection cells observed during cold air outbreaks. J. Atmos. Sci., 43, 26-39.

Schwalb, A. (1978):

The Tiros-N/NOAA A-G satellite series. NOAA Technical Memorandum, NESS 95, Washington D.C.

van Delden, A. (1986):

On cumulus cloud patterns and the theory of shallow convection. Univ. Utrecht, 1986, pp 185.